International Research Journal of Engineering and Technology (IRJET) e-ISSN: 2395-0056
Volume: 04 Issue: 07 | July -2017 www.irjet.net p-ISSN: 2395-0072

A Comparison of Closed-Loop Performance of Multirotor Configurations Using Nonlinear Dynamic Control

Mostafa Moussid[1], Alaa Bensaid[2], Adil Sayouti[3], Mostafa Radoui[4], Hicham Medromi[5]

[1,2] Doctoral student in computer engineering, the National Higher School of electricity and mechanics (ENSEM), Morocco
[3]Dr. Professor, Royal Navy School (ERN) of Morocco, Casablanca, Morocco
[4]Professor, the National Higher School of electricity and mechanics (ENSEM), Morocco
[5]Dr. Professor and Director, the National Higher School of electricity and mechanics (ENSEM), Morocco

---

Abstract - *The use of Unmanned Aerial Vehicles (UAVs) which can operate autonomously in dynamic and complex operational environments is becoming increasingly more common. During the last decade many research papers have been published on the topic of architecture, dynamic modeling and control strategies of autonomous multi rotors. This article highlights the primary differences between three multi rotor platforms: quad rotor, hexa rotor and octo rotor, a discussion is presented on the changes to the vehicle dynamics, controller and closed-loop performance as a result of augmenting the aircraft with additional rotors. The common properties of the vehicles are first presented. The differences in each configuration are then described.*

In this work a generalized dynamical model of the multi-rotor unmanned aerial vehicles (UAVs) is presented. The nonlinear dynamic model of the multi rotor is formulated using the Newton-Euler method, the formulated model is detailed including aerodynamic effects and rotor dynamics that are omitted in many literature. Based on the mathematical model, three algorithms of command have been analyzed, as backstepping, sliding-mode and a hybrid backstepping/ FST (Frenet-Serret Theory) controllers. Simulation based experiments were conducted to evaluate and compare the performance of the proposed control techniques in terms of dynamic performance, stability and the effect of possible disturbances. Finally, integral backstepping is augmented with FST (Frenet-Serret Theory) action and proposed as a tool to design attitude, altitude and position controllers. The conclusion of this work is a proposal of hybrid systems to be considered as they combine advantages from more than one control philosophy.

These developments are part of the overall project initiated by the team (EAS) of the Computer Laboratory, systems and renewable energy (LISER) of the National School of Electrical and Mechanical (ENSEM).

Key Words: **Multicopter, Nonlinear control, Newton-Euler method, PID, Backstepping, sliding-mode, Frenet-Serret Theory (FST).**

1. INTRODUCTION

Unmanned autonomous aerial vehicles have become a real center of interest. In the last few years, their utilization has significantly increased. Many research papers have been published on the topic of modeling and control strategies of autonomous multirotors.

Today, they are used for multiple tasks of civil as well as military applications, such as navigation, search and rescue mission, building exploration, surveillance, security, transportation and much more.

The multirotors are commonly used in dangerous and inaccessible environments.

This work will focus on the modeling and control of a multirotor type UAV. The reason for choosing the multirotor is in addition to its advantages (high agility and maneuverability, relatively better payload, vertical take-off and landing (VTOL) ability), the multirotor does not have complex mechanical control linkages due to the fact that it relies on fixed pitch rotors and uses the variation in motor speed for vehicle control [1].

However, these advantages come at a price as controlling a multirotor is not easy because of the coupled dynamics and its commonly under-actuated design configuration [2]. In addition, the dynamics of the multirotor are highly non-linear and several uncertainties are encountered during its missions [3], thereby making its flight controls a challenging venture. This has led to several control algorithms proposed in the literature.

The contributions of this paper are: firstly, deriving an accurate and detailed mathematical model of the multirotor UAV, developing linear and nonlinear control algorithms and applying those on the derived mathematical model in computer based simulations and to provide a valid confrontation and a comparison between four different control techniques in terms of their dynamic performance and their ability to stabilize the system under the effect of possible disturbances. The conclusion of this work is a

proposal of hybrid systems to be considered as they combine advantages from more than one control philosophy.

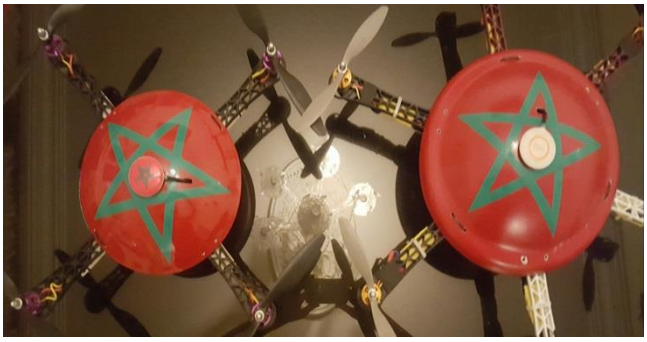

Fig -1: A picture of the developed multirotor (SMART\ENSEM)

The most popular UAV airframe types can be organized into three main categories: "fixed-wing", "multicopters" and "FW hybrid VTOL". Each category has its own advantages and disadvantages that must be considered when choosing a UAV [4].

Merging the benefits of fixed-wing UAVs with the ability to hover is a new category of hybrids which can also take off and land vertically [5].

There are various types under development, some of which are basically just existing fixed-wing designs with vertical lift motors bolted on. Others are 'tail sitter' aircraft which look like a regular plane but rest on their tails on the ground, pointing straight up for takeoff before pitching over to fly normally, or 'tilt rotor' types where the rotors or even the whole wing with propellers attached can swivel from pointing upwards for takeoff to pointing horizontally for forward flight [6].

While a new breed of superclass long range multirotor drones continues to extend its presence in the fixed wing commercial space, there is also space for both, often the best solution is a combination of both.

2. MULTIROTOR CONCEPT AND MOST COMMON CONFIGURATIONS

In this section, we address the basic, general rules in picking a multirotor configuration. The most multirotor UAVs use Conventional Configurations either 4, 6 or 8 propellers, which can be arranged in various configurations. As already mentioned above, there are many types of multirotor. They are generally categorized by the number of motors used. The number of motors and configuration has impact on flight performance. For instance the more motors, the more power (more lift capacity), which means you could carry more payload. More motors also mean better redundancy in case of motor failure. But the downside is decrease in energy efficiency, and increase in cost for purchasing additional motors and associated parts. In what follows, we will give a brief description of different configurations of the multirotor.

- Quadrotor: micro air vehicle platform, consistent four rotors mounted on a symmetric frame typically 90° x or + configuration.

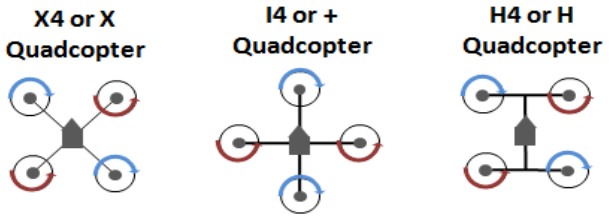

Fig -2: Quadcopter configurations

- Multirotor: Consistent of the Six Rotor mounted orthogonally along the body typically Y, H configuration

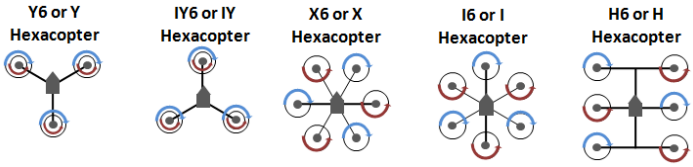

Fig -3: Hexacopter configurations

- Octorotor having a total of eight rotors mounted orthogonally along the body typically I8, I8+, V, X configuration.

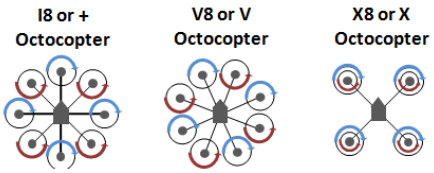

Fig -4: Octocopter configuration

The following table summarizes the performance of the five multirotor configurations described above.

Table -1: The performance of multirotor configurations.

Multicopter UAV Type	Complexity	Redundancy	Payload Capability	Cost
Bicopter	High	None	Lowest	Low
Tricopter	Medium	None	Low	Low
Quadcopter	Low	None	Medium	Medium
Hexacopter	Medium	Low	High	High
Octocopter	High	High	Highest	Highest

3. DYNAMIC MODEL OF THE MULTIROTOR

The multirotor is an under-actuated system because it has six-degree of freedom while it has only four inputs. The collective input (or throttle input) is the sum of the thrusts of each motor. The goal of this section is to define physical Equations of Motion that describes the dynamics and aerodynamics of the UAV involved. The mathematical model of the multirotor has to describe its attitude according to the well-known geometry of this UAV.

The schematic structure of the multirotor and the rotational directions of the propellers are illustrated in Figure 5. In order to describe the multirotor motion only two reference systems are necessary: earth inertial frame (R_I-frame) and body-fixed frame (R_B -frame). The airframe orientation is denoted by ${}^{B}_{I}\Re$ matrix. ${}^{B}_{I}\Re$ Stands for the rotation from R_B to R_I. The dynamic model of multirotor is derived from Newton-Euler approach.

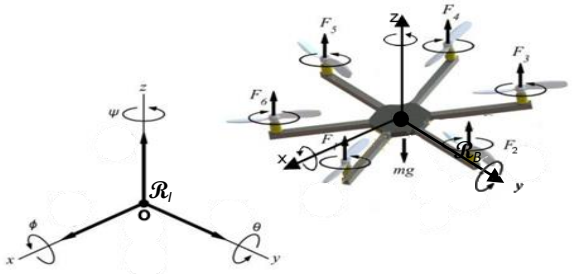

Fig -5: The structure of multirotor and its frames

Meanwhile, the Euler angles are roll angle $\emptyset \in \left]-\frac{\pi}{2},\frac{\pi}{2}\right[$, pitch angle $\theta \in \left]-\frac{\pi}{2},\frac{\pi}{2}\right[$ and yaw angle $\psi \in]-\pi,\pi[$ respectively. The rotation matrices from body frame to earth frame can be obtained as,

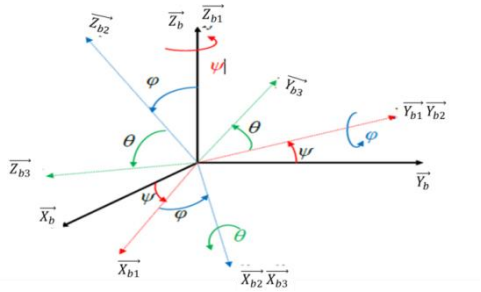

Fig -6: The orientation of the Multirotor by the Euler angles.

$$R_i^b(\emptyset,\theta,\psi) == \begin{pmatrix} C\theta C\psi & C\psi S\theta S\emptyset - S\psi C\emptyset & C\psi S\theta C\emptyset + S\psi S\emptyset \\ C\theta S\psi & S\psi S\theta S\emptyset + C\psi C\theta & S\psi S\theta C\emptyset - C\psi S\emptyset \\ -S\theta & C\theta S\emptyset & C\theta C\emptyset \end{pmatrix} \quad (1)$$

With [C: Cos and S: Sin].
And denoting ω as the angular body rate of the airframe in body-fixed frame, angular body rate and Euler angle parameterization relationship can be given as, With

$$\vec{\eta} = (\phi,\theta,\psi)^T$$

$$\dot{\vec{\eta}} = \begin{bmatrix} \dot{\emptyset} \\ \dot{\theta} \\ \dot{\psi} \end{bmatrix} = \begin{pmatrix} 1 & tg\theta sin\emptyset & tg\theta cos\emptyset \\ 0 & cos\emptyset & -sin\emptyset \\ 0 & \frac{sin\emptyset}{cos\theta} & \frac{cos\emptyset}{cos\theta} \end{pmatrix} \begin{bmatrix} p \\ q \\ r \end{bmatrix} = Q_\eta[\vec{\omega}(t)] \quad (2)$$

With:

- $\emptyset$ Rotation about x axis : $-\frac{\pi}{2} < \emptyset < \frac{\pi}{2}$ (roll).
- θ Rotation about y axis : $-\frac{\pi}{2} < \theta < \frac{\pi}{2}$ (pitch).
- ψ Rotation about y axis : $-\pi < \psi < \pi$ (yaw).

3.1 Applied forces and torques

The two main forces come from gravity and the thrust of the rotors but to make the model more realistic rotor drag and air friction is also included. The UAV rotorcraft system are quite complex. Their movements are governed by several effects either mechanical or aerodynamic. The main effects on the acting multirotor have been listed in the following table:

Table -2: The main effects on the acting multirotor

Effects	Fountainhead
Aerodynamics effects	Rotating propellers
Inertial counter torque	Speed change of propellers
Effect of gravity	Position of the center of mass
Gyroscopic effects	Change in the direction of the drone
The friction effect	All the movements of the drone

3.1.1 The Forces

- Gravity force: $\vec{P} = [0,\ 0,\ mg]^T$
- Thrust force: $\overrightarrow{Th} = R_i^b[0,\ \ 0,\ U_1 = \sum_{i=1}^{n} b\,\Omega_i^2]^T$
- Rotor drag : $\vec{Ft} = \vec{K}_{ft}\vec{V} = I_{3x3}[k_{ftx},\ \ k_{fty},\ \ k_{ftz}]^T.\dot{\vec{\xi}}$

3.1.1 The Torques

$$\text{Roll torque: } U_\phi = bl\left(\sum_{k=1}^{N} -\cos\left[(k-\delta)*\frac{2\pi}{N}\right]\Omega_k^2\right)$$

$$\text{Pitch torque: } U_\theta = bl\left(\sum_{k=1}^{N} \sin\left[(k-\delta)*\frac{2\pi}{N}\right]\Omega_k^2\right) \quad (3)$$

$$With\ \ \delta = \begin{cases} 1\ si\ la\ configuration\ "+" \\ 1/2\ si\ la\ configuration\ "X" \end{cases}$$

$$\text{Yaw torque: } U_\psi = d\left(\sum_{k=1}^{N} (-1)^{k+1}\Omega_k^2\right) \quad (4)$$

- Gyroscopic : $\overrightarrow{M}_{gh} = \sum_{i=1}^{n}\Omega_r \wedge J_r[0,\ 0,\ (-1)^{i+1}\omega_i]^T = [-J_r\dot{\theta}\Omega_r, J_r\Omega_r, 0]^T$
- Yaw counter torque : $\overrightarrow{M}_{ccl} = [0, 0, J_r\dot{\Omega}_r]^T$
- Aerody. resistance : $\overrightarrow{M}_{fa} = [K_{fax}\dot{\phi}^2, K_{fay}\dot{\theta}^2, K_{faz}\dot{\psi}^2]^T$

3.2 Hexacopter Mathematical Model

To derive the dynamic model of the multirotor (position and attitude); the Newton-Euler formalism is used [4]. Therefore the following equations are obtained:

$$\begin{pmatrix} mI_{3x3} & 0_{3x3} \\ 0_{3x3} & J \end{pmatrix}\begin{pmatrix} \dot{\vec{V}} \\ \dot{\vec{\omega}} \end{pmatrix} + \begin{pmatrix} \vec{\omega} \wedge m\vec{V} \\ \vec{\omega} \wedge J\vec{\omega} \end{pmatrix} = \begin{pmatrix} \vec{F}^B \\ \vec{M}^B \end{pmatrix} \quad (5)$$

$$\begin{cases} \dot{\vec{\xi}}(t) = \vec{V}(t) \\ m\dot{\vec{V}}(t) + \vec{\omega} \wedge m\vec{V} = \vec{F}^B \\ \dot{\vec{\eta}} = Q_\eta[\vec{\omega}(t)] \\ J\dot{\vec{\omega}}(t) + \dot{\omega}(t).J\vec{\omega}(t) = \vec{M}^B \end{cases} \quad (6)$$

The equations of motion, that governs the translational and the rotational motion for the multirotor with respect to the body frame are:

3.2.1 Translational dynamic

$$\begin{cases} \dot{\vec{\xi}}(t) = \vec{v}(t) \\ m\dot{\vec{V}}(t) + m\dot{\omega}(t).\vec{V}(t) = \vec{F}^B \end{cases} \quad (7)$$

$$\begin{cases} \ddot{X} = \frac{1}{m}[(cos\phi cos\psi sin\theta + sin\phi sin\psi)U_1 - k_{ftx}\dot{X}] \\ \ddot{Y} = \frac{1}{m}[(cos\phi sin\psi sin\theta - sin\phi cos\psi)U_1 - k_{fty}\dot{Y}] \\ \ddot{Z} = \frac{1}{m}[(cos\phi cos\theta)U_1 - k_{ftz}\dot{Z}] - g \end{cases} \quad (8)$$

With $U_x = (cos\phi cos\psi sin\theta + sin\phi sin\psi)$

$$U_y = (cos\phi sin\psi sin\theta - sin\phi cos\psi)$$

It is very important to take into consideration the non-holonomic constraints of the drone as they are in conformity with physical laws and they define the coupling of the different system states. The development of non-holonomic constraints makes it possible to explain the coupling between the different states of the system. From the equations of the translation dynamics **(8)**, the expressions of the non-holonomic constraints [29] can be extracted as follows:

$$tg(\theta) = \frac{(m\ddot{X} + k_{ftx}\dot{X})cos\psi + (m\ddot{Y} + k_{fty}\dot{Y})sin\psi}{m\ddot{Z} + k_{ftz}\dot{Z} + mg}$$

$$sin\phi = \frac{(m\ddot{X} + k_{ftx}\dot{X})sin\psi - (m\ddot{Y} + k_{fty}\dot{Y})cos\psi}{\sqrt{(m\ddot{X} + k_{ftx}\dot{X})^2 + (m\ddot{Y} + k_{fty}\dot{Y})^2 + (m\ddot{Z} + k_{ftz}\dot{Z} + mg)^2}}$$

This implies

$$\theta_d = Arctang\left[\frac{(m\ddot{X} + k_{ftx}\dot{X})cos\psi + (m\ddot{Y} + k_{fty}\dot{Y})sin\psi}{m\ddot{Z} + k_{ftz}\dot{Z} + mg}\right] \quad (9)$$

$$\phi_d = Arcsin\left[\frac{(m\ddot{X} + k_{ftx}\dot{X})sin\psi - (m\ddot{Y} + k_{fty}\dot{Y})cos\psi}{\sqrt{(m\ddot{X} + k_{ftx}\dot{X})^2 + (m\ddot{Y} + k_{fty}\dot{Y})^2 + (m\ddot{Z} + k_{ftz}\dot{Z} + mg)^2}}\right]$$

3.2.2 Rotational dynamics

$$J\dot{\vec{\omega}}(t) = \vec{M}^B - \dot{\omega}(t).J\vec{\omega}(t) \quad (10)$$

$$\begin{cases} J_{xx}\ddot{\phi} = \dot{\theta}\dot{\psi}(J_{yy} - J_{zz}) - K_{fax}\dot{\phi}^2 - J_r\Omega_r\dot{\theta} + U_\phi \\ J_{yy}\ddot{\theta} = \dot{\phi}\dot{\psi}(J_{zz} - J_{xx}) - K_{fay}\dot{\theta}^2 + J_r\Omega_r\dot{\phi} + U_\theta \\ J_{zz}\ddot{\psi} = \dot{\phi}\dot{\theta}(J_{xx} - J_{yy}) - K_{faz}\dot{\psi}^2 + J_r\dot{\Omega}_r + U_\psi \end{cases} \quad (11)$$

The multicopter's total thrust force and torque control inputs $U_1,\ U_\phi,\ U_\theta.\ U_\psi$ are related to the motor's speed by the following equations: $\vec{U} = [U_1\ \ U_\phi\ \ U_\theta\ \ U_\psi]^T$ is the vector of (artificial) input variables[5]:

$$M_{4xN} = \begin{bmatrix} b \dots\dots\dots\dots\dots & \dots\dots\dots\dots b \dots\dots\dots & \dots\dots & \dots\dots b \\ -blsin(1-\delta)\frac{2\pi}{N} \dots\dots\dots & -blsin(i-\delta)\frac{2\pi}{N} \dots & -blsin(N-\delta)\frac{2\pi}{N} & \\ -blcos(1-\delta)\frac{2\pi}{N} \dots\dots\dots & -blcos(i-\delta)\frac{2\pi}{N} \dots & -blcos(N-\delta)\frac{2\pi}{N} & \\ d \dots\dots\dots\dots\dots\dots\dots & (-1)^{i+1}d \dots\dots\dots\dots & \dots\dots & \dots -d \end{bmatrix}$$

3.3 Rotor Dynamics

The rotors are driven by DC-motors with the well-known equations:

$$\begin{cases} L\dfrac{dI(t)}{dt} = V(t) - RI(t) - k_{fcem}\Omega & \text{Electrical Equation} \\ J\dfrac{d\Omega}{dt} = C_m - C_r - f_v\Omega & \text{Mecanical Equation} \end{cases} \quad (12)$$

As we use a small motor with a very low inductance, thesecond order DC-motor dynamics may be approximated [5]:

$$\dot{\Omega} = \frac{1}{J}\left(\frac{-k_m k_{fcem}}{R} - f_v\right)\Omega - \frac{d_0}{J\eta_t r^8}\Omega^2 + \frac{k_m}{JR}V(t)$$

By introducing the propeller and the gearbox models,the equation may be rewritten:

$$\dot{\Omega} = -\frac{k_m^2}{JR}\Omega - \frac{d_0}{J\eta_t r^8}\Omega^2 + \frac{k_m}{JR}V(t) \quad (13)$$

We present our practice experience for calculate the constant (b = Thrust/RPM^2 and d=Drag/ RPM^2) in several propeller size with different rotate per minute (RPM) in multirotor. Measures of the following parameters:

Voltage, Current,Throttle input, Motor load and Speed.
The applied calculation formulas are:

- Mechanical power (W) = Torque (Nm) * Speed (rad/s)
- Electrical Power (W) = Voltage (V) * Current (A)
- Motor Efficiency = MP / EP

Fig -7: Components and measure

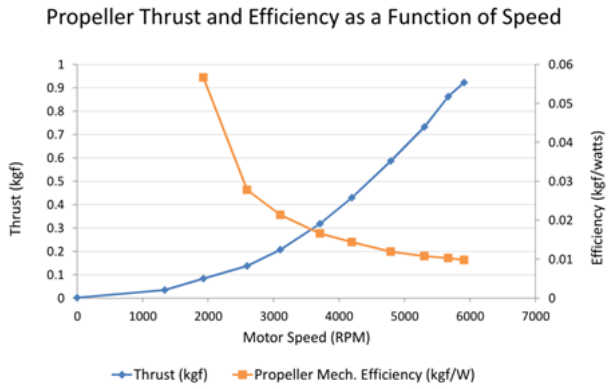

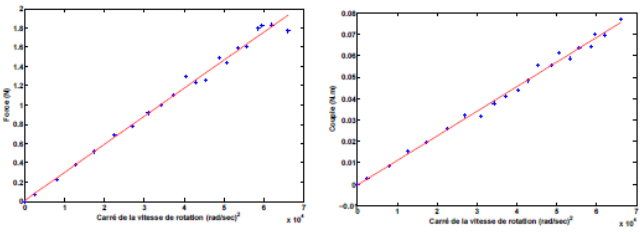

Chart -1: Determination of aerodynamic parameters

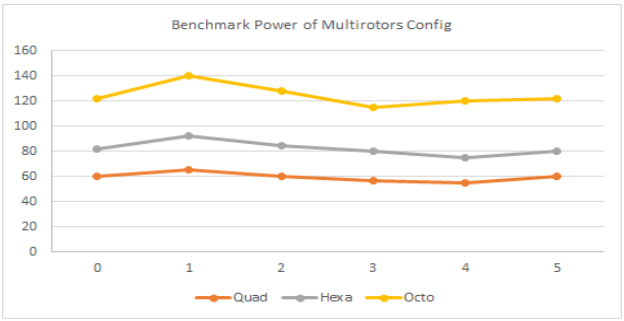

Chart -2: Benchmark Power of multirotor config

In this next section, we present the application of three different control techniques Backstepping, Sliding-mode and Backstepping+TFS to multirotor.

4. NONLINEAR CONTROLLER FOR MULTIROTOR

In this section, a Backstepping and Sliding-Mode controller are used to control the attitude, heading and altitude of the multirotor.

The Backstepping controller is based on the state space model derived in (7). Using the backstepping approach, one can synthesize the control law forcing the system to follow the desired trajectory. Refer to [6] and [7] for more details. The basic sliding mode controller design procedure is performed in two steps. Firstly, choice of sliding surface (S) is made according to the tracking error, while the second step consist the design of Lyapunov function which can satisfy the necessary sliding condition $(S\dot{S} < 0)$[9][10]. At the end the hybrid control algorithm based on a novel technique is developed during this work called: hybrid Backstepping + Frenet-Serret Theory.

4.1 Control Strategy

Due to the nature of the dynamics of the multirotor, several control algorithms have been applied to it. As to be expected, each control scheme has its advantages and disadvantages. The control schemes used could be broadly categorized as linear and non-linear control schemes. In this review a broad range of controllers within these categories are discussed.

In this section, a control strategy is based on two loops (inner loop and outer loop). The inner loop contains four control laws: roll command (ϕ), pitch command (θ), yaw control (ψ) and controlling altitude Z. The outer loop includes two control laws positions (x, y). The outer control loop generates a desired for roll movement (θ_d) and pitch (ϕ_d) through the correction block. This block corrects the rotation of roll and pitch depending on the desired yaw (ψ_d). The figure below shows the control strategy we will adopt

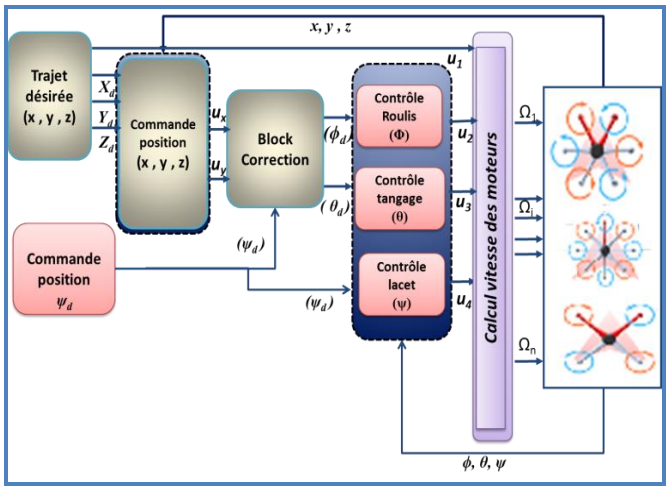

Fig -8: Synoptic scheme of the proposed control strategy

The dynamic model presented in equations set (8 and 10) can be rewritten in the state-space form $\dot{X} = f(X, U)$. $X \in R^{12}$ is the vector of state variables given as follows:

$$X^T = [\phi \ \dot{\phi} \ \theta \ \dot{\theta} \ \psi \ \dot{\psi} \ x \ \dot{x} \ y \ \dot{y} \ z \ \dot{z}]$$

$$[x_1 \ x_2 \ x_3 \ x_4 \ x_5 \ x_6 \ x_7 \ x_8 \ x_9 \ x_{10} \ x_{11} \ x_{12}]$$

$x_1=\phi$ $x_2=\dot{x}_1=\dot{\phi}$ $x_3=\theta$ $x_4=\dot{x}_3=\dot{\theta}$ $x_5=\psi$ $x_6=\dot{x}_5=\dot{\psi}$

$x_7= x$ $x_8=\dot{x}_7=\dot{x}$ $x_9= y$ $x_{10}=\dot{x}_9=\dot{y}$ $x_{11}= z$ $x_{12}=\dot{x}_{11}=\dot{z}$

$$\begin{cases} \dot{x}_2=\ddot{\phi} = a_1x_4x_6 - a_2x_2^2 - a_3\Omega_r x_4 + b_1U_\phi \\ \dot{x}_4=\ddot{\theta} = a_4x_2x_6 - a_5x_4^2 + a_6\Omega_r x_2 + b_2\,U_\theta. \\ \dot{x}_6=\ddot{\psi} = a_7x_2x_4 - a_8x_6^2 + b_3\,U_\psi. \\ \dot{x}_8=\ddot{x} = -a_9x_8 + \frac{1}{m}U_XU_1. \\ \dot{x}_{10}=\ddot{y} = -a_{10}x_{10} + \frac{1}{m}U_YU_1. \\ \dot{x}_{12}=\ddot{z} = -a_{11}x_{12} + \frac{cos\phi cos\theta}{m}U_1 - g. \end{cases} \quad (14)$$

To simplify, define,

$a_1=(J_{yy}-J_{zz})/J_{xx}$	$a_2=K_{fax}/J_{xx}$	$a_9=K_{ftx}/m$
$a_4=(J_{zz}-J_{xx})/J_{yy}$	$a_5=K_{fay}/J_{yy}$	$a_{10}=K_{fty}/m$
$a_7=(J_{xx}-J_{yy})/J_{zz}$	$a_8=K_{faz}/J_{zz}$	$a_{11}=K_{ftz}/m$
$a_3=J_r/J_{xx}$	$a_6=J_r/J_{yy}$	
$b_1=1/J_{xx}$	$b_2=1/J_{yy}$	$b_3=1/J_{zz}$

Rewriting the last equation (14) to have the angular and the translational accelerations in terms of the other variables (Rotational and translational equations of motion),

$$\begin{pmatrix} \dot{x}_2 \\ \dot{x}_4 \\ \dot{x}_6 \end{pmatrix} = \begin{pmatrix} a_1x_4x_6 - a_2x_2^2 - a_3\Omega_r x_4 + b_1U_\phi \\ a_4x_2x_6 - a_5x_4^2 + a_6\Omega_r x_2 + b_2\,U_\theta \\ a_7x_2x_4 - a_8x_6^2 + b_3\,U_\psi \end{pmatrix} \quad (15)$$

$$\begin{pmatrix} \dot{x}_8 \\ \dot{x}_{10} \\ \dot{x}_{12} \end{pmatrix} = \begin{pmatrix} -a_9x_8 + (cosx_1cos\,x_5\,sin\,x_3 + sinx_1sin\,x_5)\frac{U_1}{m} \\ -a_{10}x_{10} + (cosx_1sin\,x_3\,sin\,x_5 - sinx_1cos\,x_5)\frac{U_1}{m} \\ -a_{11}x_{12} - g + (cosx_1cos\,x_3)\frac{U_1}{m} \end{pmatrix}$$

4.2 Backstepping Controller

Using the backstepping approach, one can synthesize the control law forcing the system to follow the desired trajectory. Refer to [7] and [8] for more details.

4.2.1 Backstepping of the Rotations Subsystem

$$U_\phi=\frac{1}{b1}[-a_1x_4x_6 - a_2x_2^2 - a_3\Omega_r x_4 + \ddot{\phi}_d + k_1(-k_1e_1+e_2) + k_2\,e_2 + e_1]$$
$$U_\theta=\frac{1}{b2}[-a_4x_2x_6 - a_5x_4^2 - a_6\Omega_r x_2 + \ddot{\theta}_d + k_3(-k_3e_3+e_4) + k_4\,e_4 + e_3] \quad (16)$$
$$U_\psi=\frac{1}{b3}[-a_7x_2x_4 - a_8x_6^2 + \ddot{\psi}_d + k_5(-k_5e_5+e_6) + k_6\,e_6 + e_5]$$

4.2.2 Backstepping of the Linear Translations

The altitude control U_1 and the Linear (U_x, U_y) Motion Control are obtained using the same approach described in my article [11].

$$U_1=\frac{m}{cosx1cos\,x3}[g - a_{11}x_{12} + \ddot{z}_d + k_{11}(-k_{11}e_{11}+e_{12}) + k_{12}\,e_{12} + e_{11}]$$

$$U_X=\left(\frac{m}{U_1}\right)[-a_9x_8 + \ddot{x}_d + k_7(-k_7e_7+e_8) + k_8\,e_8 + e_7] \quad (17)$$

$$U_Y=\left(\frac{m}{U_1}\right)[-a_{10}x_{10} + \ddot{y}_d + k_9(-k_9e_9+e_{10}) + k_{10}\,e_{10} + e_9].$$

4.3 Sliding mode control

The basic sliding mode controller design procedure is performed in two steps. Firstly, choice of sliding surface (S) is made according to the tracking error, while the second step consist the design of Lyapunov function which can satisfy the necessary sliding condition $(S\dot{S}<0)$ [9],[10].

$$U_\phi=\frac{1}{b1}[-a_1 x_4 x_6 - a_2 x_4\Omega_r+\ddot{\phi}_d+\lambda_1 e_2- k_1 sign(S_\phi)] \quad \text{(Roll)}$$

$$U_\theta=\frac{1}{b2}[-a_3 x_2 x_6 - a_4 x_2\Omega_r+\ddot{\theta}_d+\lambda_2 e_4- k_2 sign(S_\theta)] \quad \text{(Pitch)}$$

$$U_\psi=\frac{1}{b3}[-a_5 x_2 x_4 - a_4 x_2\Omega_r+\ddot{\psi}_d+\lambda_3 e_6- k_3 sign(S_\psi)] \quad \text{(Yaw)} \quad \textbf{(18)}$$

$$U_1=\frac{m}{\cos x1 \cos x3}[g+\ddot{z}_d+\lambda_4 e_8- k_4 sign(S_z)] \quad \text{(Altitude)}$$

$$U_X=\left(\frac{m}{U_1}\right)[\ddot{x}_d+\lambda_5 e_{10}- k_5 sign(S_x)] \quad \text{(Linear x Motion)}$$

$$U_Y=\left(\frac{m}{U_1}\right)[\ddot{y}_d+\lambda_6 e_{12}- k_6 sign(S_y)] \quad \text{(Linear y Motion)}$$

The sliding mode control inputs which were derived and expressed in equation (15) were applied to the nonlinear model in (18) and responses are shown in fig. 9.

4.4 Control Using Backstepping+FST Technique

To increase robustness (to external disturbances) of the general backstepping algorithm, the Backstepping + FST control results from the merge of the Frenet-Serret Theory [11] and the integral backstepping technique.

As shown in Figure 9, the complete system control is composed by a cascade-connection of altitude, position and attitude controllers. However, attitude control is the heart of the control system, which maintains the UAVs stable and oriented towards the desired direction. This section shows *roll*- control derivation based on hybrid backstepping and the Frenet-Serret equations previously introduced.

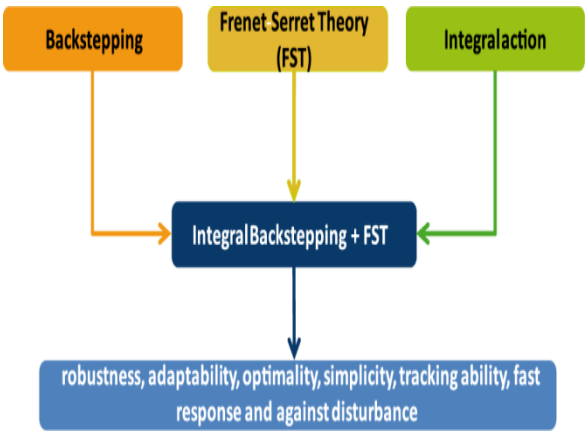

Fig -9: The Proposed control approach

Consider the *roll* tracking error e_ϕ and its dynamics:

$$e_\phi = (\dot{\phi}_d - \phi) \text{ and } \dot{e}_\phi = (\dot{\phi}_d - \omega_x)$$

A Lyapunov function:

$$V(e_\phi)=\frac{1}{2}e_\phi^2; \text{ then } \dot{V}(e_\phi)=e_\phi(\dot{\phi}_d-\omega_x)$$

The angular velocity ω_x is not our control input, hence we must define a virtual control that fulfill with desired system behavior. The virtual control law for stabilizing the angular tracking error e_2 is then defined as:

$$e_2=\omega_{xd}-\omega_x$$
$$\omega_{xd}=\dot{\phi}_d+\alpha_\phi e_\phi+\lambda_\phi\int e_\phi(\tau)d\tau \qquad (\alpha_\phi \text{ and } \lambda_\phi>0)$$

$$\Longrightarrow \dot{e}_2=\alpha_\phi\dot{e}_\phi+\ddot{\phi}_d+\lambda_\phi e_\phi-\ddot{\phi}=\alpha_\phi(\omega_{xd}-\omega_x)+\ddot{\phi}_d+\lambda_\phi e_\phi-\ddot{\phi}$$

With $\dot{e}_\phi=-\alpha_\phi e_\phi+\lambda_\phi\int e_\phi(\tau)d\tau+e_2$

$$\Longrightarrow \dot{e}_2=\alpha_\phi(-\alpha_\phi e_\phi+\lambda_\phi\int e_\phi(\tau)d\tau+e_2)+\ddot{\phi}_d+\lambda_\phi e_\phi-\ddot{\phi} \quad \textbf{(19)}$$

4.5 Attitude control

$$\dot{e}_2=\alpha_\phi(-\alpha_\phi e_\phi+\lambda_\phi\int e_\phi(\tau)d\tau+e_2)+\ddot{\phi}_d+\lambda_\phi e_\phi-(a_1 x_4 x_6 + a_2 x_2^2 + a_3\Omega_r x_4 + b_1 U_\phi).$$

Solving this equation which is the control law for achieving *roll* stabilization being the desirable dynamics for the angular speed tracking error $\dot{e}_2=-e_\phi-\lambda_2 e_2$:

The control input U_ϕ is then extracted, satisfying:

$$U_\phi=\frac{1}{b1}[\alpha_\phi(-\alpha_\phi e_\phi+\lambda_\phi\int e_\phi(\tau)d\tau+e_2)+\ddot{\phi}_d+\lambda_\phi e_\phi-a_1\dot{\theta}\dot{\psi}+ - a_2\dot{\phi}^2 - a_3\Omega_r\dot{\theta}+e_\phi+\lambda_2 e_2]$$

$$U_\phi=\frac{1}{b1}[e_\phi(1+\lambda_\phi-\alpha_\phi^2)+e_2(\alpha_\phi+\lambda_2)+\alpha_\phi\lambda_\phi\int e_\phi(\tau)d\tau+\ddot{\phi}_d-a_1\dot{\theta}\dot{\psi}+ - a_2\dot{\phi}^2 - a_3\Omega_r\dot{\theta}].$$

Where $(\alpha_\phi, \lambda_\phi \text{ and } \lambda_2)>0$ are the control parameters of the backstepping +FST method.

Pitch and yaw control is derived by applying the same procedure. Control laws are:

$$U_\phi=\frac{1}{b1}[e_\phi(1+\lambda_\phi-\alpha_\phi^2)+e_2(\alpha_\phi+\lambda_2)+\alpha_\phi\lambda_\phi\int e_\phi(\tau)d\tau+\ddot{\phi}_d-a_1\dot{\theta}\dot{\psi}+ - a_2\dot{\phi}^2 - a_3\Omega_r\dot{\theta}]. \quad \textbf{(20)}$$

$$U_\theta=\frac{1}{b1}[e_\theta(1+\lambda_\theta-\alpha_\theta^2)+e_3(\alpha_\theta+\lambda_3)+\alpha_\theta\lambda_\theta\int e_\theta(\tau)d\tau+\ddot{\theta}_d-a_4\dot{\phi}\dot{\theta}-a_5\dot{\theta}^2- +a_6\Omega_r\dot{\phi}].$$

$$U_\psi=\frac{1}{b1}[e_\psi(1+\lambda_\psi-\alpha_\psi^2)+e_4(\alpha_\psi+\lambda_4)+\alpha_\psi\lambda_\psi\int e_\psi(\tau)d\tau+\ddot{\psi}_d-a_7\dot{\phi}\dot{\theta}- a_8\dot{\psi}^2].$$

4.6 Altitude control

Using the same procedure showed in the previous subsection, altitude tracking error and its dynamics are:

$$e_z = \varepsilon_d - \varepsilon$$

$$e_5 = \alpha_z e_z + \lambda_z \int e_z(\tau)d\tau + \dot{e}_z$$

$$U_1 = \frac{m}{\cos\theta\cos\phi}[g - a_{11}\dot{z} + e_z(1+\lambda_z - \alpha_z^2) + e_5(\alpha_z+\lambda_5) + \alpha_z\lambda_z\int e_z(\tau)d\tau]$$

where (α_z, λ_z and λ_5)> 0 are the control parameters of the backstepping +FST method.

4.6.1 Position control

$$e_x = x_d - x \qquad e_6 = \alpha_x e_x + \lambda_x \int e_x(\tau)d\tau + \dot{e}_x$$

$$e_y = y_d - y \qquad e_7 = \alpha_y e_y + \lambda_y \int e_y(\tau)d\tau + \dot{e}_y$$

Control laws are then introduced in Equation,

$$U_X = \left(\frac{m}{\theta}\right)[e_x(1+\lambda_x - \alpha_x^2) + e_6(\alpha_x+\lambda_6) - \alpha_x\lambda_x\int e_x(\tau)d\tau] \qquad \textbf{(21)}$$

$$U_Y = \left(\frac{m}{\phi}\right)[e_y(1+\lambda_y - \alpha_y^2) + e_7(\alpha_y+\lambda_7) - \alpha_y\lambda_y\int e_y(\tau)d\tau].$$

Where (α_x, α_y, λ_x , λ_y , λ_6, λ_7)> 0.

Equations (19 to 21) show the Backstepping + FST methodology. The aim of addressing a new term within the single backstepping was to make the control effort more energetic in terms of angular response. This new term, called $\ddot{\phi}_d$ corresponds to a desired acceleration function that strictly depends on the velocity and acceleration of the vehicle. As already mentioned, the Frenet Serret formulas were used to obtain that function.

5. SIMULATION RESULTS

A complete simulation was then implemented on MATLAB/Simulink relying on the derived mathematical model of multirotor. The simulation environnement was added to evoluate the mentioned controllers and compare their dynamic performances under different types of input conditions.

Table -3 Numerical values used in simulations

	Quadrotor	Hexarotor	Octorotor	Unit
m	0.65	0.468	1.2	Kg
l	0.23	0.225	0.4	m
b	$3.13.10^{-5}$	$2.9\ 10^{-6}$	$3.13\ 10^{-5}$	Kg.m
d	$7.5.10^{-7}$	$1.14\ 10^{-7}$	$7.5.10^{-7}$	Kg.m^2
I_{xx}	$7.5\ 10^{-3}$	$4.85\ 10^{-3}$	$7.5\ 10^{-3}$	Kg.m^2
I_{xx}	$7.5\ 10^{-3}$	$4.85\ 10^{-3}$	$7.5\ 10^{-3}$	Kg.m^2
I_{xx}	$1.3\ 10^{-2}$	$8.15\ 10^{-3}$	$1.3\ 10^{-2}$	Kg.m^2
I_{xx}	$6\ 10^{-5}$	$3.36\ 10^{-5}$	$6\ 10^{-5}$	Kg.m^2

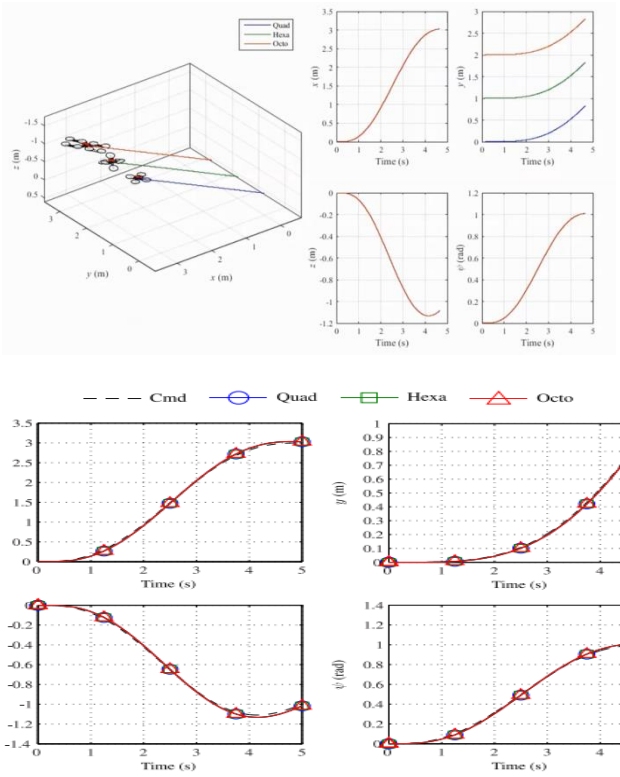

Chart -3: Dynamic response in position / heading for each multirotor

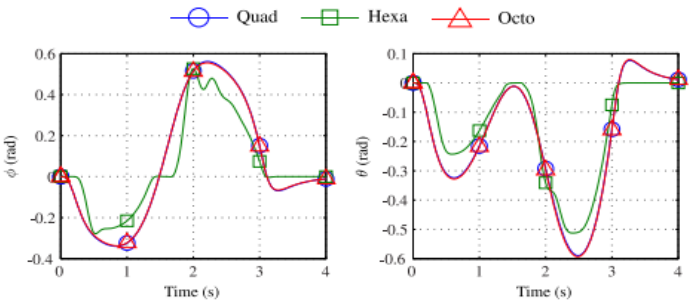

Chart -4: Dynamic response in roll and pitch

Dynamic reponse in position heading, Roll and Pitch for each multirotor when accuratlly tracking commanded path. The SMC and Backstepping controllers gave better performance outside the linear hovering region due to their nonlinear nature.

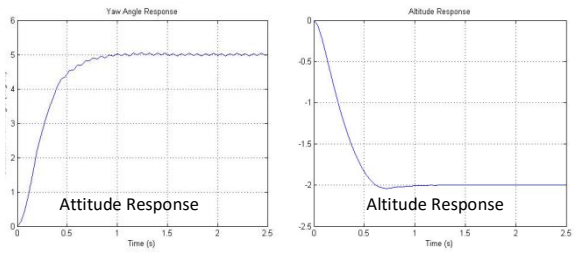

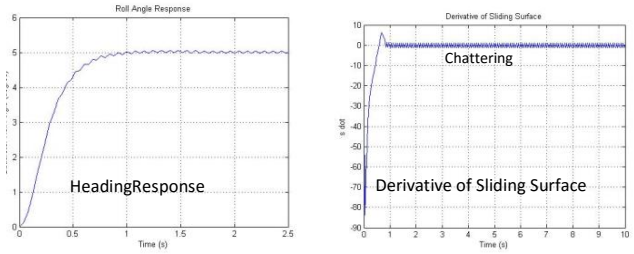

Chart -5: The slidingControl Simulation Response

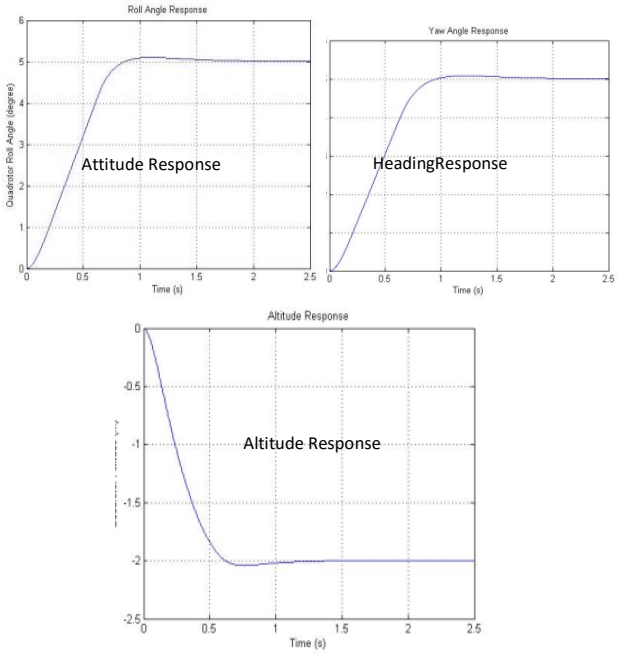

Chart -6: The Backstepping Control Simulation Response

To be able to compare fairly between the three implemented control techniques, the response graph of the system under the effect of each the three controllers was plotted superimposed on one another.

Chart -7 shows the altitude response, the attitude and heading responses respectively.

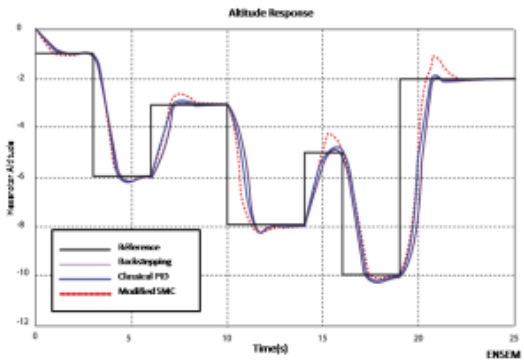

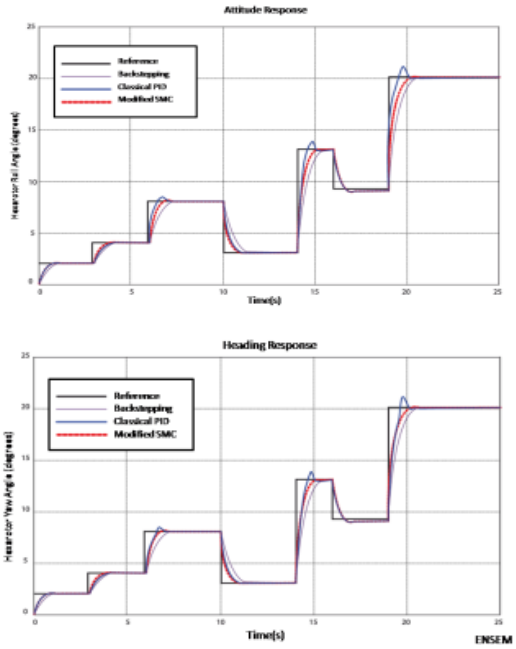

Chart -7: The altitude, the attitude and heading responses

4. RESULTS AND DISCUSSION

In this paper, three different controllers are presented for the attitude, altitude and heading of a multirotor. The first control technique is the Backstepping, its ability to control the orientation angles in presence of relatively high perturbations is very interesting. To increase robustness (to external disturbances) of the general backstepping algorithm, an integrator is added and the algorithm becomes Integrator backstepping control. The integral approach was shown to eliminate the steady-state errors of the system, reduce response time and restrain overshoot of the control parameters. The second one is the sliding-mode technique SMC. It was well enough to stably drive the multirotor to a desired position, but it did not provide excellent results. This controller has the problem of chattering, the switching nature of the controller seems to be ill adapted to the dynamics of the multirotor. The third, last but not least, the hybrid control algorithms based on a novel technique developed during this work called: hybrid Backstepping + Frenet-Serret Theory. This controller supports on existing backstepping methodology but adopts the FST formulation that allows introducing a desired attitude angle acceleration function dependent on multirotor acceleration. Consequently, improvements on disturbance rejection and attitude tracking are achieved against other classical techniques.

As evident from the review, no single algorithm presents the best of the required features. It was found out, in recent literature, that using only one type of flight control algorithms was not sufficient to guarantee a good performance, especially when the multirotor is not flying near its nominal condition.

It also been discussed that getting the best performance usually requires hybrid control schemes that have the best combination of robustness, adaptability, tracking ability, optimality, fast response, simplicity and disturbance rejection among other factors. However, such hybrid systems do not guarantee good performance; hence a compromise needs to be found for any control application on which of the factors would be most appropriate.

In table.3 summarizes the comparison of the various algorithms as applied to multirotor with all things being equal. The performance of a particular algorithm depends on many factors that may not even be modeled. Hence, this table serves as guide in accordance with what is presented in this work and common knowledge ([12], [13])

TABLE -4 Comparisons of multirotor control algorithms.

Characteristic	SMC	BS	BS+FST
Robust	A	LN	A
Adaptive	H	H	H
Optimal	A	LN	LN
Intelligent	LN	LN	A
Tracking ability	H	H	H
Fast convergence	H	LN	A
Precision	H	A	A
Simplicity	A	LN	LN
Disturbance rejection	H	H	H
Noise (signal)	LN	LN	A
Chattering	H	LN	LN

Legend: **LN**—low to none; **A**—average; **H**—high.

5. CONCLUSIONS AND FUTURE WORKS

The goal of this work was to derive a mathematical model for the multirotor Unmanned Aerial Vehicle (UAV) and develop nonlinear control algorithms to stabilize the states of the multirotor, which include its altitude, attitude, heading and position in space and to verify the performance of these controllers with comparisons via computer simulations. The mathematical model of a multirotor UAV was developed in details including its aerodynamic effects and rotor dynamics which we found lacking in many literatures; a review of the popular controllers proposed for the multirotor systems is developed. An important part of this work was dedicated to finding a good control approach for multirotor. Three techniques were explored from theoretical development to final experiments. As evident from the review, no single algorithm presents the best of the required features. It also been discussed that getting the best performance usually requires hybrid control schemes that have the best combination of robustness, adaptability, optimality, simplicity, tracking ability, fast response and disturbance rejection among other factors.

The integral Backstepping + FST control was used as an approach for attitude control (Integral Backstepping + Frenet-Serret Theory). This controller supports on existing backstepping methodology but adopts the FST formulation that allows introducing a desired attitude angle acceleration function dependent on multirotor acceleration. Consequently, improvements on disturbance rejection and attitude tracking are achieved against other classical techniques. Thus, integral backstepping+FST have been proposed for full control of multirotor.

Our future work is to implementing the developed control techniques on real hexarotor hardware to give a more fair comparison between their performances. The development of novel control strategies and methodologies for improving the level of autonomy of miniature flying vehicles remains under current research. The research in the Computer Laboratory, systems and renewable energy (LISER) of the National School of Electrical and Mechanical (ENSEM) is continuing toward implementing these algorithms in real time.

The positive results achieved through this development enhance our knowledge of this very unstable system and encourages us to continue towards full autonomy multirotor.

REFERENCES

[1] Huo, X., Huo, M. and Karimi, H.R. (2014) Attitude Stabilization Control of a Quadrotor UAV by Using Backstepping Approach. Mathematical Problems in Engineering, 2014, 1-9.

[2] Mahony, R., Kumar, V. and Corke, P. (2012) Multirotor Aerial Vehicles: Modeling, Estimation, and Control of Quadrotor. RoboticsAutomationMagazine,19,20-32.

[3] Lee, B.-Y., Lee, H.-I. andTahk, M.-J. (2013) Analysis of adaptive Control Using On-Line Neural Networks for a Quadrotor UAV.13th International Conference on Control, Automation and Systems (ICCAS), 20-23 October 2013, 1840- 1844.

[4] Simon János, Goran Martinovic, Navigation of Mobile Robots Using WSN's RSSI Parameter and Potential Field Method, ActaPolytechnicaHungarica, Journal of Applied Sciences Vol.10, No.4,pp. 107-118, 2013.

[5] Jun Shen, Qiang Wu, Xuwen Li, Yanhua Zhang, Research of the RealTime Performance of Operating System, 5th International conference on Wireless Communications, Networking and Mobile Computing, pp. 1-4, 2009.

[6] R. M. Murray and S. S. Sastry, A mathematical introduction to robotic manip-ulation. CRC press, 1994.

[7] A.W.A. Saif, M. Dhaifullah, M.A.Malki and M.E. Shafie,"ModiffiedBackstepping Control of Quadrotor", InternationalMulti-Conference on System, Signal and Devices, 2012.

[8] A.A. Main, W. Daobo, "Modeling and Backstepping-basedNonlinear Control Strategy for a 6 DOF Quadrotor

Helicopter",Chinese Journal of Aeronautics 21, pp. 261-268, 2008.

[9] V.G. Adir, A.M.Stoica and J.F. Whidborne, "Sliding ModeControl of 4Y Octorotor", U.P.B. Sci. Bull., Series D, Vol.74,Iss. 4, pp. 37-51,2012.

[10] K. Runcharoon and V. Srichatrapimuk, "Sliding Mode Control ofQuadrotor" International Conference of TechnologicalAdvances in Electrical, Electronics and Computer Engineering,pp. 552-556 May 9-11, 2013.

[11] M.Moussid, A.Sayouti and H. Medroumi, "Autonomous HexaRotor Arial Dynamic Modeling and a Review of Control Algorithms" E-ISSN: 2395-0056. VOLUME: 02 ISSUE: 05 AUG-2015.

[12] Cetinsoy, E., Dikyar, S., Hancer, C., Oner, K.T., Sirimoglu, E., Unel, M. and Aksit, M.F. (2012) Design and Construction of a Novel Quad Tilt-Wing UAV. Mechatronics, 22, 723-745.

[13] Senkul, F. and Altug, E. (2013) Modeling and Control of a Novel Tilt-Roll Rotor Quadrotor UAV. Proceedings of the 2013 International Conference on Unmanned Aircraft Systems (ICUAS), Atlanta, 28-31 May 2013, 1071-1076.

[14] Zeghlache, S., Saigaa, D., Kara, K., Harrag, A. and Bouguerra, A. (2012) Backstepping Sliding Mode Controller Im- proved with Fuzzy Logic: Application to the Quadrotor Helicopter. Archives of Control Sciences, 22, 315-342.

[15] Benallegue, A., Mokhtari, A. and Fridman, L. (2006) Feedback Linearization and High Order Sliding Mode Observer for a Quadrotor UAV. Proceedings of the International Workshop on Variable Structure Systems, Alghero, 5-7 June 2006, 365-372.

[16] Madani, T. and Benallegue, A. (2008) Adaptive Control via Backstepping Technique and Neural Networks of a Quadrotor Helicopter. Proceedings of the 17th World Congress of the International Federation of Automatic Control, Seoul, July 6-11 2008, 6513-6518.

BIOGRAPHIES

Mostafa Moussid Doctoral student in computer engineering of the National Higher School of electricity and mechanics (ENSEM), Morocco.

Alaa Bensaid Doctoral student in computer engineering of the National Higher School of electricity and mechanics (ENSEM), Morocco.

Mostafa RADOUI received his PHD in informatics in 1985 professor at the ENSEM in Casablanca and member of engineering science research team and the system architecture of ENSEM.

Adil Sayouti received the PhD in computer science from the ENSEM, Hassan II University in July 2009, Morocco. In 2003, he obtained the Microsoft Certified Systems Engineer.

Hicham Medromi received the PhD in engineering science from the Sophia Antipolis University in 1996, Nice, France. He is director of the National Higher School of electricity and Mechanics, Hassan II University Morocco